A NEW METHOD FOR HEART RATE MONITORING DURING PHYSICAL EXERCISE USING PHOTOPLETHYSMOGRAPHIC SIGNALS

Tim Schäck, Christian Sledz, Michael Muma, Abdelhak M. Zoubir

Signal Processing Group
Technische Universität Darmstadt
Merckstr. 25, 64283 Darmstadt, Germany

ABSTRACT

Accurate and reliable estimation of the heart rate using wearable devices, especially during physical exercise, must deal with noisy signals that contain motion artifacts. We present an approach that is based on photoplethysmographic (PPG) signals which are measured with two wrist–type pulse oximeters. The heart rate is related to intensity changes of the reflected light. Our proposed method suppresses the motion artifacts by adaptively estimating the transfer functions of each of the three–axis acceleration signals that produce the artifacts in the PPG signals. We combined the output of the six adaptive filters into a single enhanced time–frequency domain signal based on which we track the heart rate with a high accuracy. Our approach is real–time capable, computationally efficient and real data results for a benchmark data set illustrate the superior performance compared to a recently proposed approach.

***Index Terms*—** Photoplethysmography (PPG), Heart Rate Monitoring, Adaptive Filters, Accelerometer, Time–Frequency, Noise Reduction, Motion Artifacts

1. INTRODUCTION

Wearable devices that contain optical heart rate monitors are an emerging technology that can be used, e.g as a tool to control the training load during physical exercises or to monitor physiologic conditions during daily activities. In contrast to the previous generation of devices, it is no longer necessary to wear an additional chest strap, since the heart rate is monitored from the wrist by means of photoplethysmography (PPG).

PPG [1] refers to a noninvasive indirect measurement of the blood flow. Pulse oximeters illuminate the skin along with underlying blood vessels via light-emitting diodes (LEDs) to measure intensity changes of the reflected light that is absorbed by the photo diodes. Based on the intensity change in the PPG signal, the arterial oxygen saturation and the heart rate can be estimated. Combining the PPG signal with an electrocardiogram (ECG), allows for deriving additional parameters, such as, e.g. the pulse arrival time (PAT) which is correlated with the blood pressure [2].

However, the PPG measurement is susceptible to motion artifacts (MA), which inevitable occur during physical exercises. Motion induced artifacts can strongly deteriorate the quality of a PPG signal and signal processing techniques are required to remove the MA from the PPG signal prior to estimating the heart rate.

In recent years, different approaches on how to clean the PPG signals from MA have been proposed. In [3], three synthetic noise reference signals are generated internally from the artifact contaminated PPG signal itself. The reference signals were constructed from singular value decomposition (SVD), fast Fourier transform (FFT), and independent component analysis (ICA) and are applied to the adaptive step-size least mean squares (AS-LMS) filter for artifact removal. However, this method is limited by the sensitivity to the reference signal, which is not able to represent all real-world characteristics, especially during various forms of physical exercise.

ICA was also used in [4], where motion artifacts were reduced by exploiting the quasi-periodicity of PPG signal and the independence between the PPG and the motion artifact signals via a combination of ICA and block interleaving. Krishnan et al. [5] propose a frequency domain ICA routine that is more effective in artifact removing than time-domain ICA. However, ICA based approaches rely on the assumption of statistical independence of motion artifacts and arterial volume variations, which could not be confirmed by Yao and Warren [6].

In order to model the influence of motion to the PPG signals, other approaches use adaptive filter algorithms and acceleration data as a motion reference [7–9]. However, all of these methods were examined for small movements and the PPG sensors were placed at the finger ring or forehead and not at the wearer's wrist. The performance during physical exercises is expected to decrease.

Zhang et al. [10] proposed a framework for heart rate monitoring during intensive physical exercise consisting of signal decomposition, sparse signal reconstruction and spectral peak tracking with verification. However, this approach is computationally demanding and may not work on real-time fitness devices or may consume to much battery power.

978-0-9928626-3-3/15/$31.00 ©2015 IEEE

Our contribution lies in proposing a new algorithm for heart rate monitoring based on PPG and acceleration signals that is both highly accurate and low in computational cost. The proposed method for heart rate monitoring is based on a set of adaptive filters that estimate the effects of motion in the PPG signal. By combining all filter outputs in the time–frequency domain, we are able to track the heart rate based on an enhanced signal. We show that our method outperforms previous work on a reference data set.

The remainder of the paper is organized as follows: First, Section 2 presents the signal model used in this work. Our method is proposed in Section 3, followed by the description of the data set and the results in Section 4. Finally, a conclusion is given in Section 5.

2. SIGNAL MODEL

In this paper, we propose the following measurement model:

$$p(n) = s(n) + m(n) + v(n) \tag{1}$$

Here, $p(n)$ is the measured PPG signal, $s(n)$ is the noise-free PPG signal which is sought for, $m(n)$ are the motion induced artifacts and $v(n) \sim \mathcal{N}(0, \sigma^2)$ represents the sensor and amplifier noise. We next model the effects of the motion artifacts $m(n)$ in dependence of the measured three channel acceleration signal vector $\mathbf{a}(n)$ by introducing a time-varying system with impulse response $h(n, \alpha, \omega, \psi)$ and rewrite the model using matrix notation:

$$p(n) = s(n) + \mathbf{h}^T(n, \alpha, \omega, \psi)\mathbf{a}(n) + v(n) \tag{2}$$

The impulse response $\mathbf{h}(n, \alpha, \omega, \psi)$ is assumed to be non-stationary, i.e., it depends on the time index n. Additionally, it also depends on the variable α, which is the acceleration that acts on the sensor, the angular velocity for rotational movements ω, and the actual position of the sensor ψ.

As in practice the angular velocity ω and the actual position ψ is not always available, we restrict the model to the acceleration α. Hence, the system model equation simplifies to

$$p(n) = s(n) + \mathbf{h}^T(n, \alpha)\mathbf{a}(n) + v(n). \tag{3}$$

3. PROPOSED METHOD

The proposed approach is based on three consecutive steps: First, the non-stationary impulse response $\mathbf{h}(n, \alpha)$ is estimated and the linear influence of the acceleration, which acts on the PPG sensor, to the noise-free PPG signal is removed. This estimation process is accomplished by an adaptive filter that minimizes the difference between the measured PPG and acceleration signal. Second, a signal enhancement is performed based on the adaptive filter outputs, where non-coherent noise components are suppressed by element–wise multiplication of the resulting spectrograms. Finally, a heart rate tracker follows the most probable high energy continuous line in the spectrogram. An overview of the proposed algorithm is provided in Fig. 2.

3.1. Adaptive Filtering of PPG Signals from Accelerometer Signals

In the first part, the motion artifact suppression by use of adaptive filters is explained. First, a general topology for artifact suppression via adaptive filters is derived and the optimization criterion is defined. Then, the applied adaptive NLMS filter is described.

3.1.1. General Topology

The adaptive filter minimizes the power of acceleration signal components in the PPG signal, i.e., it maximizes the signal-to-motion artifact ratio (SMR). Based on this approach, we derive the difference equation

$$e(n) = p(n) - \hat{m}(n), \tag{4}$$

where $e(n)$ is the error signal, $p(n)$ is the measured PPG signal and $\hat{m}(n)$ is the estimated motion artifact caused by the acceleration. The adaptive filter structure is visualized in Fig. 1.

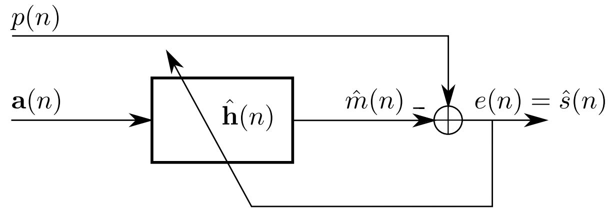

Fig. 1. Adaptive filter structure for removal of motion artifacts.

We can now transform (4) into vector-matrix notation and replace the estimated motion artifact $\hat{m}(n)$ by the product of the estimated impulse response $\hat{\mathbf{h}}(n, \alpha)$ and the measured acceleration vector $\mathbf{a}(n)$:

$$e(n) = p(n) - \hat{\mathbf{h}}^T(n, \alpha)\mathbf{a}(n), \tag{5}$$

Here, the error signal $e(n)$ is, in fact, an estimate of the desired original PPG signal $\hat{s}(n)$ without motion artifacts. In our approach, each PPG signal is combined with every dimension of the three-axis acceleration signal, yielding six adaptive filters that operate in parallel, see Fig. 2.

In our work, we applied different kinds of adaptive filters, such as, e.g. the Kalman filter [11, 12], the Kalman smoother [7], the least mean square (LMS) [8, 13], the normalized least mean square (NLMS) filter [7], or the adaptive step-size least mean squares (AS-LMS) filter [14]. The Kalman filter achieved similar results as the NLMS filter but required more than double of the computational time. The standard formulation of the Kalman smoother can be used

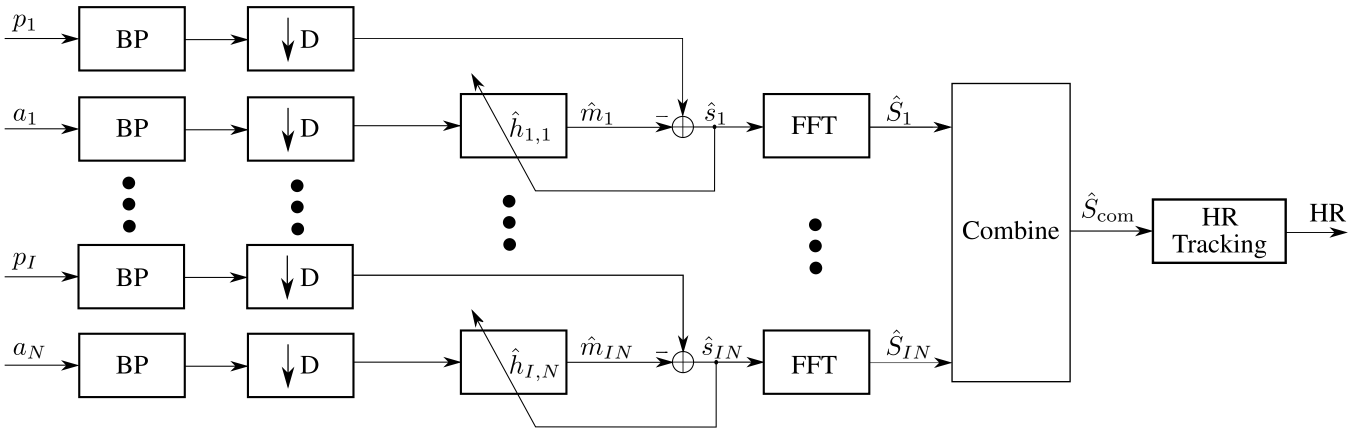

Fig. 2. Overview of the proposed algorithm with $I = 2$ PPG signals and $N = 3$ acceleration signals, which results in $IN = 6$ adaptive filters. The inputs of the adaptive filters are bandpass (BP) filtered and downsampled by a factor D to reduce computational cost. The weighted combination is performed on the spectrograms which are efficiently computed by means of the FFT. Based on the combination of the spectrograms, the heart rate can be estimated and tracked in the final step. In this figure, the time and frequency indices are left out for the sake of clarity.

only after data acquisition is complete but not for real-time processing. Based on the normalization, the step-size value $\mu \in [0, 1]$ within the NLMS filter can be formulated much easier compared to the LMS filter. Finally, due to the low computational complexity $\mathcal{O}(N)$ and the requirement of a fast adaptive algorithm for real-time purposes, we recommend the use of the NLMS and only report the results for this filter due to page restrictions.

3.1.2. Normalized Least Mean Square (NLMS) Filter

The objective of the LMS filter minimize the mean square error min $\mathsf{E}[|e(n)|^2]$. For a better control of the step-size μ, we compute the filter weights of the NLMS filter as follows:

$$\hat{\mathbf{h}}(n+1) = \hat{\mathbf{h}}(n, \alpha) + \frac{\mu}{\mathbf{a}^T(n)\mathbf{a}(n) + \delta}\mathbf{a}(n)e(n) \qquad (6)$$

The value $\delta = 10^{-12}$ is added in practice for numerical stability reasons.

3.2. Signal Enhancement by Combination

The adaptive filtering provides estimates $\hat{s}_i(n)$, $i = 1, \ldots, 6$ of the desired original PPG signal without motion artifacts. At this point, the estimates need to be combined in a reasonable manner. This is done in order to remove all incoherent components, such as, e.g. the high noise floor, and enhance coherent components like those related to the heart rate.

For all six estimates of $s(n)$, the time-varying spectrum is estimated via the short-term Fourier transform (STFT). The combination of the six time-varying spectra is done by a computationally efficient and simple element–wise multiplication of the spectrograms. This multiplication leads to a lower noise floor level which is useful in order to extract the heart rate signal. We can formulate this as

$$\hat{S}_{\text{com}}(n, f) = \sqrt[6]{\prod_{i=1}^{6} \hat{S}_i(n, f)}, \qquad (7)$$

where $\hat{S}_{\text{com}}(n, f)$ is the combined spectrogram dependent on the time index n and the frequency band index f. The variable $\hat{S}_i(n, f)$ corresponds to the channel i.

3.3. Heart Rate Tracking

The last step in the proposed algorithm is the actual heart rate (HR) estimation. This estimation is based on a extremely simple tracker that follows the most probable high energy continuous line in the enhanced spectrogram $\hat{S}_{\text{com}}(n, f)$. The frequency region, in which the highest energy is to be found, lies in an interval of ± 14 beats per minute (BPM) of the preceding HR estimate. As an initialization for the first few estimates, simply the highest energy in the frequency region from $40 - 170$ BPM is selected.

To prevent the tracking algorithm from losing the HR over a long time, the ratio between the highest peak in the observed frequency region and the highest peak in an interval of ± 100 BPM of the preceding HR estimate is calculated and compared to a predefined threshold T,

$$\frac{\max\{\hat{S}_{\text{com}}(n, \Delta f_{100})\}}{\max\{\hat{S}_{\text{com}}(n, \Delta f_{14})\}} > T. \qquad (8)$$

If the threshold T is exceeded, for example, if the algorithm had mistakenly tracked a non-stationary high power transient noise that lost its energy, it switches to the alternative high energy value in the frequency neighborhood.

4. RESULTS

We use a real data set consisting of 12 measurements that was recorded by [10]. Each data set consists of a two-channel PPG signal, a three-axis acceleration signal, and an ECG signal. The sampling rate for all signals is 125 Hz. The 12 male subjects are between 18 and 35 years old. The PPG signals were recorded from a subject's wrist using a pulse oximeter with green LED. The ECG was measured to determine the ground truth heart rate and we used the ground truth provided by the authors of [10] to evaluate our approach.

	S 1	S 2	S 3	S 4	S 5	S 6	S 7	S 8	S 9	S 10	S 11	S 12	Mean AAE
Proposed Approach	2.40	1.21	1.20	1.22	1.34	1.44	1.16	1.04	1.18	5.33	2.18	1.52	**1.77**
(SSA+FOCUSS+Vrf) [10]	2.29	2.19	2.00	2.15	2.01	2.76	1.67	1.93	1.86	4.70	1.72	2.84	**2.34**

Table 1. Average absolute error (AAE) over all 12 subjects in BPM. The second row was obtained by [10] using singular spectrum analysis (SSA), focal underdetermined system solver (FOCUSS), and verification (Vrf).

The proposed algorithm was constructed to work on sliding windows of 8 seconds and provides a new HR estimate every other second. This way, it is able to monitor the HR in real-time which is a common requirement for many applications, such as, e.g. for athletes to adjust their training program during the exercise.

The bandpass filter has a lower and upper center frequency of 0.6875 Hz resp. 10 Hz, the downsampling rate D equals 6, the NLMS filter order is set to 9, the step size μ is chosen to be 0.1, the frequency resolution of the FFT is fixed to 4096 bins and the ratio threshold for the HR tracking is determined to be $T = 5{,}000$.

The performance measurement index is the average absolute error (AAE), which is defined as

$$\text{AAE} = \frac{1}{N} \sum_{i=1}^{N} |\text{BPM}_{\text{est}}(i) - \text{BPM}_{\text{true}}(i)|, \tag{9}$$

where N is the total number of estimates, $\text{BPM}_{\text{true}}(i)$ denotes the ground truth of the HR value in the i-th time window in terms of BPM, and $\text{BPM}_{\text{est}}(i)$ denotes the corresponding estimate in BPM.

Table 1 lists the AAE for each subject's recording and gives an overall average AAE. Except for Subject 1, 10, and 11, the proposed approach outperforms the reference method on each subject. Furthermore we achieve better average performance. The average AAE across the 12 subjects is 1.77 ± 1.20 BPM (mean $\pm$ standard deviation). The best estimate is obtained for Subject 8 with 1.04 BPM on average and the worst estimate is, similar to [10], for Subject 10 with 5.33 BPM on average. In Table 1, the green color indicates the best and the red color the worst result of each method. The best and worst result of our method including the ground truth is examplarily shown in Fig. 3 superimposed on the combined spectrogram $S_{\text{com}}(n, f)$.

5. CONCLUSION

A new, effective heart rate estimator based on PPG and acceleration signals that is able to monitor a subject's heart rate in real-time during physical exercise, was presented. Our approach is based on adaptive filters, which reduce the influence of motion artifacts in the measured PPG signals. To enhance the spectral quality, we combined the outputs of the adaptive filters. Finally, a constrained heart rate tracker follows the most probable high energy continuous line in the spectrogram. Real data experiments showed an increased accu-

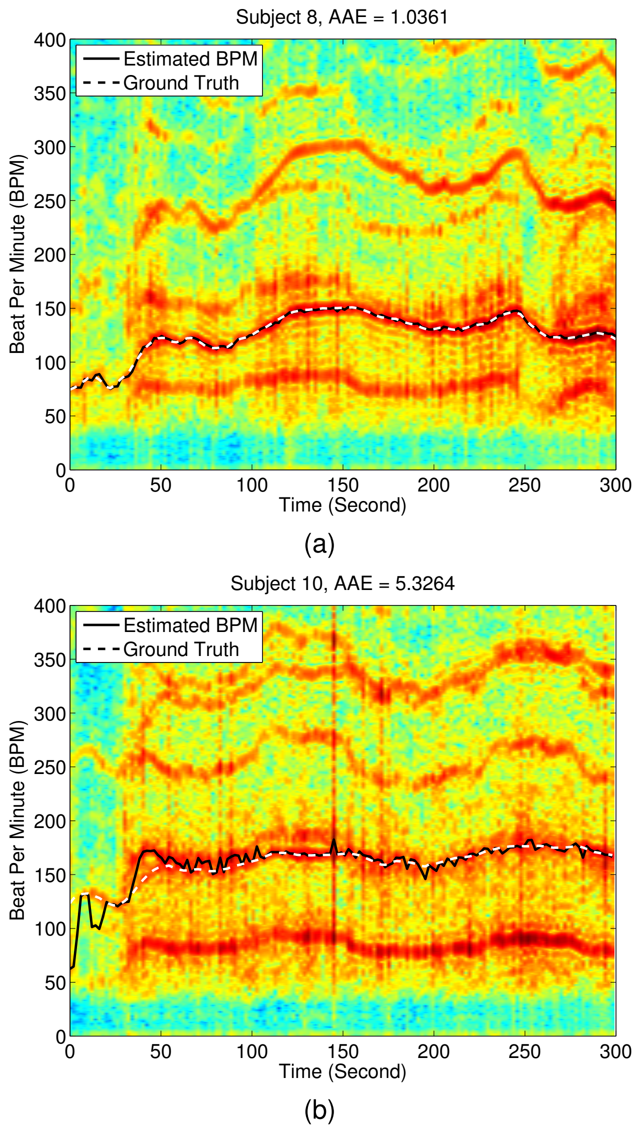

Fig. 3. Heart rate estimates depicted together with the ground truth on the combined spectrogram of all six adaptive filter outputs for (a) the best result and (b) the worst result.

racy compared to a recently published reference. Future and ongoing work include a real-time spectral quality assessment based weighted combination of the six spectrograms, which is able to account for different spectral qualities in the channels. Other tracking approaches, such as, e.g. a tracker based on autocorrelation or a multi-peak tracker, that takes the harmonic structure of the PPG into account, could also be considered and applied to the signals. However, the results that we present here were achieved by the simple outlined tracking algorithm described above.

REFERENCES

[1] J. Allen, "Photoplethysmography and its application in clinical physiological measurement," *Physiol. Meas.*, vol. 28, no. 3, pp. R1–R39, 2007.

[2] H. J. Baek, K. K. Kim, J. S. Kim, B. Lee, and K. S. Park, "Enhancing the estimation of blood pressure using pulse arrival time and two confounding factors," *Physiol. Meas.*, vol. 31, no. 2, pp. 145–157, 2010.

[3] M. R. Ram, K. V. Madhav, E. H. Krishna, K. N. Reddy, and K. A. Reddy, "A novel approach for motion artifact reduction in PPG signals based on AS-LMS adaptive filter," *IEEE Trans. Instrum. Meas.*, vol. 61, no. 5, pp. 1445–1457, May 2012.

[4] B. S. Kim and S. K. Yoo, "Motion artifact reduction in photoplethysmography using independent component analysis," *IEEE Trans. Biomed. Eng.*, vol. 53, no. 3, pp. 566–568, Mar. 2006.

[5] R. Krishnan, B. Natarajan, and S. Warren, "Two-stage approach for detection and reduction of motion artifacts in photoplethysmographic data," *IEEE Trans. Biomed. Eng.*, vol. 57, no. 8, pp. 1867–1876, Aug. 2010.

[6] J. Yao and S. Warren, "A short study to assess the potential of independent component analysis for motion artifact separation in wearable pulse oximeter signals," in *Proc. Eng. Med. Biol. Soc. IEEE EMBS 27th Annu. Int. Conf.*, 2005, pp. 3585–3588.

[7] B. Lee, J. Han, H. J. Baek, J. H. Shin, K. S. Park, and W. J. Yi, "Improved elimination of motion artifacts from a photoplethysmographic signal using a Kalman smoother with simultaneous accelerometry," *Physiol. Meas.*, vol. 31, no. 12, pp. 1585–1603, 2010.

[8] S. H. Kim, D. W. Ryoo, and C. Bae, "Adaptive noise cancellation using accelerometers for the PPG signal from forehead," in *Proc. Eng. Med. Biol. Soc. IEEE EMBS 29th Annu. Int. Conf.* IEEE, 2007, pp. 2564–2567.

[9] L. B. Wood and H. H. Asada, "Noise cancellation model validation for reduced motion artifact wearable PPG sensors using MEMS accelerometers," in *Proc. Eng. Med. Biol. Soc. IEEE EMBS 28th Annu. Int. Conf.* IEEE, 2006, pp. 3525–3528.

[10] Z. Zhang, Z. Pi, and B. Liu, "TROIKA: A general framework for heart rate monitoring using wrist-type photoplethysmographic signals during intensive physical exercise," *IEEE Trans. Biomed. Eng.*, vol. 62, no. 2, pp. 522–531, Feb. 2015.

[11] R. E. Kalman et al., "A new approach to linear filtering and prediction problems," *Trans. ASME J. Basic Eng.*, vol. 82, no. 1, pp. 35–45, 1960.

[12] S. Seyedtabaii and L. Seyedtabaii, "Kalman filter based adaptive reduction of motion artifact from photoplethysmographic signal," *Int. J. Elect. Compu. Eng.*, vol. 27, pp. 597–600, 2008.

[13] E. Hänsler, *Statistische Signale: Grundlagen und Anwendungen*, 3rd ed. Berlin Heidelberg, Germany: Springer, 3 edition, 2001.

[14] M. R. Ram, K. V. Madhav, E. H. Krishna, K. N. Reddy, and K. A. Reddy, "On the performance of AS-LMS based adaptive filter for reduction of motion artifacts from PPG signals," in *Proc. 28th IEEE Instrum. Meas. Technol. Conf. (I2MTC)*, Binjiang, China, 2011, pp. 1536–1539.